Available online at www.sciencedirect.com

SciVerse ScienceDirect

Physics Procedia 42 (2013) 206 – 212

Physics Procedia

PNCMI 2012 - Polarized Neutrons for Condensed Matter Investigations 2012

Wide Angle Polarization Analysis With Neutron Spin Filters

Q. Ye[a,b], T. R. Gentile[b], J. Anderson[b], C. Broholm[c,b], W. C. Chen[b,d], Z. DeLand[f], R. W. Erwin[b], C. B. Fu[e,b], J. Fuller[b], A. Kirchhoff[b], J. A. Rodriguez-Rivera[b,d], V. Thampy[c], T.G. Walker[f], S. Watson[b]

[a] *Oak Ridge National Laboratory, Oak Ridge, TN 37831, USA*
[b] *National Institute of Standards and Technology, Gaithersburg, Maryland, 20899, USA*
[c] *Johns Hopkins University, Baltimore, MD 21218, USA*
[d] *University of Maryland, College Park, Maryland, 20742, USA*
[e] *Indiana University, Bloomington, IN 47405, USA*
[f] *University of Wisconsin - Madison, Madison, Wisconsin 53706 USA*

Abstract

We report substantial improvements in a compact wide angle neutron spin filter system that was recently employed on the Multi-Axis Crystal Spectrometer at the Center for Neutron Research at the U.S. National Institute of Standards and Technology. The apparatus consists of a cylindrical ^{3}He polarizer cell and wide-angle ^{3}He analyzer cells, a vertical solenoid to provide a uniform magnetic field, and a shielded radio-frequency solenoid for the polarizer cell. Nuclear magnetic resonance is employed to reverse the polarization in the polarizer cell and monitor the ^{3}He polarization in all cells. The first experiment using this apparatus was carried out with cylindrical analyzer cells with limited angular coverage due to low polarizations in fused quartz cells. We present results for aluminosilicate glass analyzer cells that cover 110 ° and have long relaxation times (100 h to 400 h). Using two 100 W diode bars spectrally narrowed with chirped volume Bragg gratings, we have obtained 65 % - 80 % ^{3}He polarization in these cells. The ^{3}He polarization has been measured by neutron transmission and electron paramagnetic resonance. Additional progress includes an improved holding field solenoid and decreased spin-flip losses.

Selection and peer-review under responsibility of the Organizing Committee of the 9th International Workshop on Polarised Neutrons in Condensed Matter Investigations

Keywords: Polarized ^{3}He; ^{3}He neutron spin filter; Wide angle ^{3}He cell.

1. Introduction

Neutron spin filters (NSFs) based on polarized ^{3}He are becoming routinely used for polarized neutron research, such as for applications that either require larger solid angle coverage than that provided by supermirrors or to decouple polarization selection from energy selection on thermal neutron instruments [1, 2]. Surmounting the larger challenge of wide-angle polarization analysis would substantially increase the impact of spin filters on polarized neutron scattering and thus is currently being pursued with spin filters based on metastability-exchange optical pumping (MEOP) [3, 4, 5] and spin-exchange optical pumping (SEOP) [6]. The Multi-Axis Crystal Spectrometer (MACS) [7] at the U.S. National Institute of Standards and Technology Center for Neutron Research (NCNR) is able to simultaneously detect neutrons from twenty independent channels covering an angular range of 220 ° around the sample

Email address: qiang.ye@nist.gov (Q. Ye)

Selection and peer-review under responsibility of the Organizing Committee of the 9th International Workshop on Polarised Neutrons in Condensed Matter Investigations
doi:10.1016/j.phpro.2013.03.197

region, yielding more than an order of magnitude gain in detection efficiency as compared to a conventional triple axis spectrometer. To perform polarized neutron scattering experiments with the MACS and other instruments, analyzers covering wide scattering angles are required.

A compact system based on polarized ^{3}He neutron spin filters to retrofit MACS with neutron polarization analysis has recently been reported [6]. The concept and techniques will be applied to other instruments at the NCNR and other neutron facilities. Fig. 1 shows a schematic of the MACS sample area with the sample and three neutron spin filters inside a solenoid that provides a vertical holding field of up to 3 mT as well as the guide field for incoming and outgoing polarized neutrons. The neutron polarization is perpendicular to the scattering plane. Two wide angle ^{3}He analyzer cells covering a total of 220 ° are located between the sample and the detectors. The ^{3}He polarization in the cells is controlled and/or monitored by nuclear magnetic resonance (NMR) methods; adiabatic fast passage (AFP) is used to invert the ^{3}He polarization in the polarizer cell and free induction decay (FID) is used to monitor the polarization in all cells. The radio-frequency (RF) field for the AFP is provided by a small solenoid that is surrounded by an aluminum box to contain the RF field. Each cell's relaxation time (T_1) is monitored using a small pickup coil located on the tip-off of the cell.

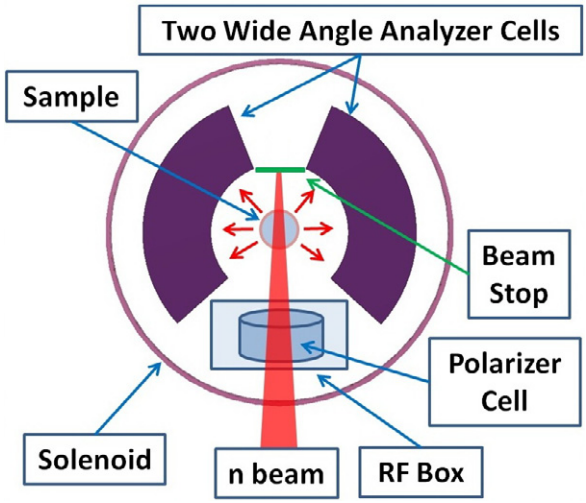

Fig. 1. Top view of the layout of the spin filter apparatus in the MACS sample area. Cold neutrons incident on the sample are polarized by a polarized ^{3}He cell that is located in an RF solenoid surrounded by an aluminum shielding box. After scattering from the sample, neutrons are detected after passing through wide angle analyzer cells.

Due to the difficulty in making complex cells from GE180 [8] glass, the work in Ref. [6] employed wide angle cells made from fused quartz. Although relaxation times of 200 h were obtained at room temperature, an unexpected temperature dependence limited the relaxation time and thus the achievable polarization under SEOP conditions. Hence in the first polarized neutron scattering experiment on a sample of FeSeTe using this apparatus conducted in Nov. 2010 [9], cylindrical GE180 cells allowing for only 35 ° of angular coverage were employed. The five-day run required swapping of polarizer and analyzer cells every one to two days. The initial ^{3}He polarizations in the two polarizer cells and two analyzer cells employed were between 69 % and 78 %, and the relaxation times were between 50 h and 94 h. The relaxation times were reduced from their intrinsic values of 100 h to 200 h due to additional magnetic field gradients from magnetic materials in the MACS system.

Here we report substantial improvements in all aspects of the MACS polarized neutron scattering apparatus, in particular the fabrication of GE180 wide-angle cells that achieve both long relaxation times and high ^{3}He polarizations. In Sec. 2 we present the fabrication method and results for these new cells. The neutron transmission measurements and electron paramagnetic resonance (EPR) to determine the polarization in these cells are discussed in Sec. 3. In Sec. 4 we describe a new, static field solenoid and improved RF spin flip efficiency as well as smaller RF leakage to

the analyzer cells. Preliminary results of studies of the temperature dependent relaxation that limits the achievable polarization in fused quartz cells are presented in Sec. 5.

2. Cell Fabrication Procedures and Results

We have successfully developed a method to fabricate wide-angle cells blown from GE180 glass. In the first step, an 8 cm diameter, ≈25 cm long, blown GE180 glass cylinder is produced from 25 mm GE180 tubing. The cylinder is then cut into three pieces at two angles of 70 ° and 110 ° with respect to the axis of the cylinder. All three pieces are fused together at high temperatures with the two ends reversed by 180 ° in a special oven. Fig. 2 shows six GE180 wide angle cells denoted by "Veronica", "Archie", "Reggie", "Jughead", "Reliance" and "Giant".

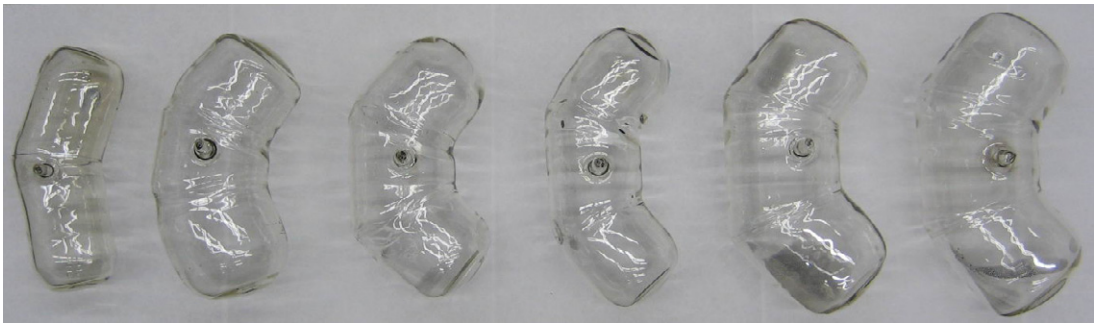

Fig. 2. Six wide angle cells denoted by "Veronica", "Archie", "Reggie", "Jughead", "Reliance" and "Giant", from left to right. The cell Veronica was the first test of the fabrication method and is made from only two sections of GE180 glass, whereas the other cells are made from three sections.

Table 1. Parameters for each wide-angle cell: name; volume V; inner diameter l, which is the path length for the neutron beam; refill status; pressure p; K/Rb vapor mixture ratio D; angular coverage; spin-up time constant T_p; longitudinal relaxation time T_1; cell opacity $n\sigma l$; and ^{3}He polarization P_{He}, where n is the ^{3}He density and σ is the unpolarized absorption cross section at a neutron wavelength of 0.381 nm. The opacity and P_{He} values listed were determined from neutron transmission measurements. Dashes indicate measurements not yet performed. The numbers in parentheses are the uncertainties in the last digits. The uncertainties in the opacity and P_{He} are limited primarily by neutron counting statistics and estimated empty cell transmission. A typical empty cell transmission is 0.88(1). As discussed in the text, the T_1 for the optically pumped/reversed orientations of the cell are listed.

Cell Name	V(cm^3)	l(cm)	Refilled	p(bar)	D@100°C	Angle	T_p(h)	T_1(h)	$n\sigma l$	P_{He}
Veronica	510	5.8	Y	1.37	1.8	90°	8.6	98/140	2.21(2)	0.80(1)
Archie	960	8.2	Y	1.17	1.8	90°	10.1	122/170	2.70(2)	0.76(1)
Reggie	830	7.2	N	1.26	1.9	110°	9.1	105/157	2.57(2)	0.76(1)
Jughead	710	6.7	N	1.34	7.8	120°	11.5	104/170	2.57(2)	0.65(1)
Reliance	1145	8.1	Y	1.16	2.1	120°	7.8	227/237	2.68(2)	0.72(1)
Giant	1290	8.2	Y	1.13	0.9	120°	9.0	394/394	-	-

The parameters for the six wide angle cells tested to date are listed in Table 1. The cells were prepared using techniques discussed elsewhere [10]. For these cells we typically did not get a sufficiently long relaxation time upon the first filling of the cell, hence we have noted in which cases the cells have been refilled. Refilling is performed because we have found that it can often lead to an improvement in relaxation time; it involves a complete repeat of the preparation procedure. In addition, the relatively low polarization in the cell Jughead may be due to a high mixture ratio [11], hence we will refill it.

The cells are optically pumped in an oven constructed from high temperature Garolite [12], polytetrafluoroethylene (PTFE) and glass. Two 100 W, single-bar diode lasers [13], each spectrally narrowed with a chirped volume Bragg grating (VBG) [14], were used to optical pump each wide angle cell from both directions (from above and below the

page in Fig. 2). For each laser, a cylindrical lens with a focal length of −100 mm was used for horizontal expansion over a distance of ≈ 1 m to fully illuminate the cell. With each laser bar operating at 95 A, a total of 120 W of narrow-band (linewidth of 0.25 nm) laser light was delivered to the cell. The ^{3}He polarization P_{He} was determined from both neutron transmission measurements and EPR (see Sec. 3). Orientation dependence [15] in the relaxation times of these cells has been observed. Usually a shorter T_1 is obtained in the optically pumped direction in the oven. Although we would prefer no orientation dependence, we will install the cell in the MACS solenoid in the orientation that yields the longer T_1 on the instrument.

3. ^{3}He polarization measurements

Neutron transmission measurements[16] were performed using the monochromatic neutron beam with a wavelength of 0.381 nm on beamline NG6A at the NCNR. Each polarized wide angle cell was transferred from the polarizing station to NG6A using a battery-powered solenoid and into a 4-coil system used to maintain the polarization of the cell during the measurement. The neutron beam diameter was limited by a 2 mm by 2 mm aperture and passed through a cross section of the wide-angle cell. A well shielded ^{3}He detector was employed to detect the neutrons after the cell. A solenoid powered by AC (alternating current) was used to depolarize the cell *in situ* and the unpolarized transmission was determined. Finally the cell was taken out of the beam and the neutron count rate was measured. The opacity and ^{3}He polarization values in Table 1 were determined from these measurements.

Motivated by the long shutdown of the NCNR reactor in 2011, we established the capability to determine the ^{3}He polarization by measuring the shift in the alkali metal's EPR frequency due to the magnetic field from the ^{3}He magnetization [17]. This capability was employed to confirm the neutron-based ^{3}He polarization values. During the EPR measurement, the intensity of a collimated portion of the optical pumping laser beam passing through the center of the ^{3}He cell was monitored by a photodiode. An EPR coil was mounted on top of the SEOP oven, ≈ 3 cm from the cell. A proportional-integral (PI) feedback box was used to lock the frequency of the EPR coil to the actual EPR frequency. To reduce sensitivity to magnetic field drifts, the EPR frequency was determined before and after inverting P_{He} using frequency sweep AFP.

The measured frequency shift is proportional to the ^{3}He number density, P_{He}, and a dimensionless constant $\kappa_{\mathrm{eff}}=\kappa_0+\kappa'$, where κ_0 depends weakly on the temperature of the cell and κ' is a relatively small correction that depends on the geometry of the cell [18]. The value of κ' is given by $\frac{3}{8\pi}C(\vec{x})-1$, where $C(\vec{x}) = B_{\mathrm{He}}(\vec{x})/M_{\mathrm{He}}$ is the ratio of the magnetic field from the polarized ^{3}He to the magnetization of the ^{3}He. $C(\vec{x})$ must be averaged along the path of the laser light that is detected by the photodiode. Although an analytical expression can be employed for cylindrical cells [19], the irregular geometry of the wide-angle cell requires a numerical evaluation of $C(\vec{x})$ as previously reported for double-cell geometries [20, 21]. We employed finite element modeling software [22] to evaluate $C(\vec{x})$ along the laser light path for wide-angle cells. For cylindrical cells the results agreed with the analytical results very well, confirming the modeling. The value of $C(\vec{x})$ is typically 6.7 for the existing wide angle cells, which yields $\kappa' = -0.20$. For comparison, κ' can vary between -0.4 and 0.2 for typical cylindrical cells, depending on whether the cell is configured for end pumping (laser light traveling along the cylindrical axis) or side pumping (laser light traveling perpendicular to the cylindrical axis).

The ^{3}He polarization results from EPR agree with the neutron-based values to within 1 %. The typical uncertainty of 3 % in the EPR results arises mainly from uncertainty in the frequency shift measurement, the ^{3}He density determination, and κ_{eff}. The ^{3}He density used in the EPR polarization calculation was based on the opacity determined from neutron transmission measurements, hence there is a correlated uncertainty.

4. Static field and shielded RF solenoids

Constructing a large, neutron-compatible solenoid presents technical difficulties due to the requirement of thin, fragile insulation on aluminum wire. A new 36 cm diameter, 75 cm long, solenoid was constructed primarily to address the winding density issues in the first MACS solenoid [6]. To prevent electrical contact between the wires and the welded aluminum support tube, the tube was anodized after construction and wrapped in one layer of 0.05 mm thick polytetrafluoroethylene (PTFE) film. Most importantly, 442 turns of special anodized aluminum wire with a

0.05 mm thick PTFE coating was wound entirely by hand for the solenoid and its end compensating coils, which successfully avoided shorts between neighboring windings. Furthermore, a gradient-field Maxwell coil (distance between the coils is $\sqrt{3}$ times the radius) was wound outside the MACS solenoid to allow for optimization of the magnetic field homogeneity on the MACS instrument. Although the MACS instrument was designed to be sufficiently non-magnetic for the operation of high-field, superconducting magnets, it still contains magnetic materials that distort the field of the static field solenoid. Use of superconducting magnets compound the problem by magnetizing these materials. Using the transverse relaxation time for FID signals, we determined that the Maxwell coil can be used to reduce applied gradients similar to those we have encountered on MACS.

The RF leakage from the shielded RF solenoid [6] generated polarization loss in the analyzer cells which was measured to be 0.6 % per spin flip when the distance from the edge of the RF box was 5 mm. To reduce this number, an additional RF box cover made from 3.2 mm thick aluminum covering the edges of the RF box was installed outside the existing RF box. (Fig. 3). The cover was essentially a five-surface rectangular box that was made from a solid

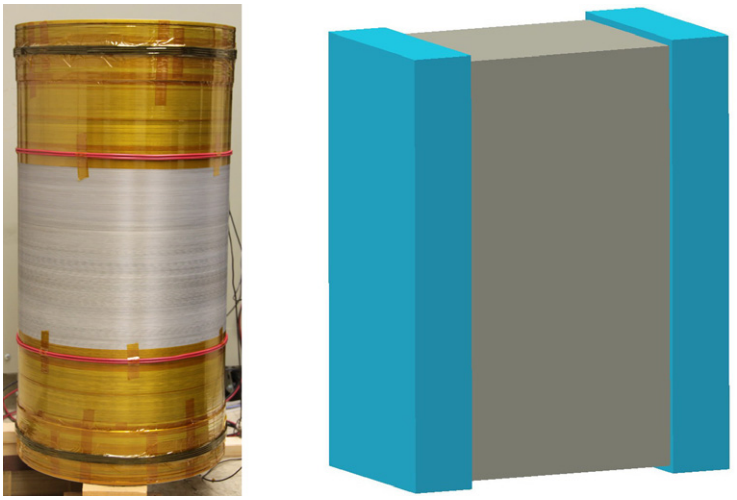

Fig. 3. New MACS solenoid entirely hand wound using PTFE coated, anodized, aluminum wire. The picture on the right shows two RF box covers (blue) made from 3.2 mm thick aluminum that cover the leakage paths at the edges of the RF box.

piece of aluminum to prevent additional RF leakage at the junction of surfaces on the original box. An amplitude modulated frequency sweep method [23] was also employed to flip the spins of the polarizer. A data acquisition card [24] was used to generate a frequency sweep across the resonance frequency while amplitude modulated by a Gaussian function. In an off-line test with the edge of the analyzer cell only 1 mm from the RF box cover, we measured a loss of 0.03 % per spin flip for the polarizer cell and 0.006 % per flip in the analyzer cell. The amplitude modulated frequency sweep was also incorporated in the EPR measurements to flip the spins of ^{3}He with little polarization loss.

5. Relaxation Studies in Quartz Cells

In [6], quartz cells (denoted by Jersey and Jekyll) were fabricated with lifetimes of $\approx$ 200 h but failed to achieve polarizations higher than 47%. The total ^{3}He relaxation rate can be represented by $\Gamma_{He} = k_{se}[Rb](1+X)+\Gamma_r$ [25], where k_{se} is the spin exchange rate coefficient, [Rb] is the Rb number density, Γ_r is the room temperature ^{3}He relaxation rate, and X is a phenomenological parameter that describes the excess relaxation typically observed in SEOP cells. In this formulation, the intercept of a plot of $\Gamma_{He} - \Gamma_r$ vs. [Rb] should be a straight line passing through the origin. This assumes that the only temperature dependence in the relaxation is through [Rb] and yields $P_{He} = P_{Rb}k_{se}[Rb]/\Gamma_{He}$. If there is any other increase in relaxation with temperature, as previously reported [26], the behavior of Γ_{He} will not be linear and the ^{3}He polarization will be decreased. As previously discussed [6], the low achievable polarizations we observed in fused quartz cells were thought to be due to the same temperature dependence observed in Ref. [26].

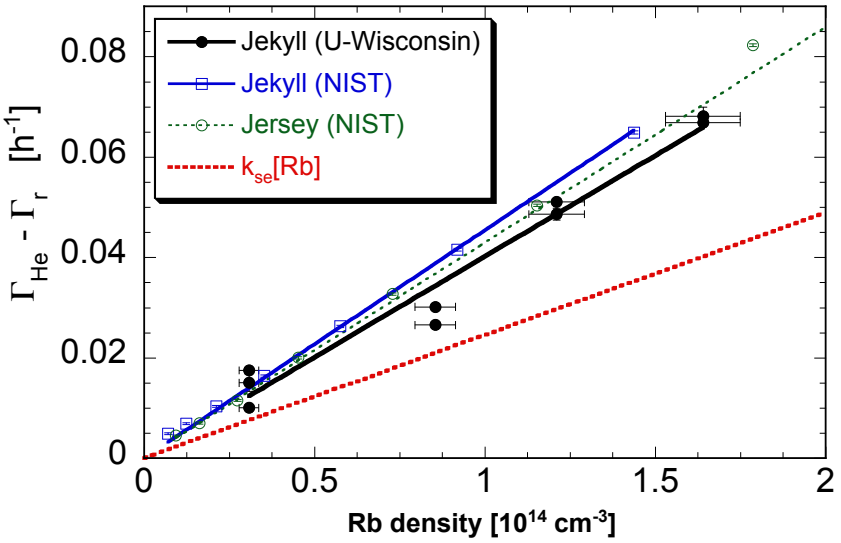

Fig. 4. $\Gamma_{He} - \Gamma_r$ for measurements of the temperature dependence of relaxation for the quartz cells Jekyll (Univ. of Wisconsin and NIST data shown by solid black circles and open blue squares, respectively) and Jersey (NIST data shown by open green circles). Values for [Rb] were determined as discussed in the text. Error bars not visible are smaller than the size of the points. The solid lines show linear fits to the data for each cell with the intercepts fixed at zero. The dotted red line shows the Rb spin-exchange rate k_{se}[Rb].

In order to further understand this behavior, we measured the temperature dependence of the relaxation time for the cells Jersey and Jekyll. Jersey is a three-section wide angle cell and Jekyll is a two-section cylindrical cell. As shown in Fig. 4, we found a linear dependence for the variation of $\Gamma_{He} - \Gamma_r$ with an intercept close to zero, indicating little additional temperature dependence in Γ_{He} besides that proportional to [Rb]. At NIST $\Gamma_r = 1/213$ h^{-1} and $\Gamma_r = 1/73.7$ h^{-1} were measured for Jersey and Jekyll, respectively. [Rb] was determined from vapor pressure curves [27] based on a thermal sensor that was located near the wide-angle cell. To check for possible error in the evaluation of [Rb], we measured the initial polarizing rate, which is given by $\gamma_{se} P_{Rb}$. Assuming P_{Rb}=1, the measured value of (0.044 ± 0.004) h^{-1} at a measured temperature of 175 °C implied an actual temperature of (161.8±1.8) °C. Hence we made a constant fractional correction to the measured temperatures of 8.5 % to evaluate the Rb density, which yielded $X = 0.85 \pm 0.18$ for Jekyll and $X = 0.75 \pm 0.17$ for Jersey. The uncertainties arise primarily from uncertainty in the temperature correction, which changes the slope of the fitted lines for the NIST data in Fig. 4.

Due to concerns about uncertainties in the determination of [Rb], these results were confirmed with measurements for the cell Jekyll at the Univ. of Wisconsin. For these data, the densities were determined directly by Faraday rotation[28] and confirmed by transmission measurements. These data are also shown in Fig. 4 and yield a linear dependence on $\Gamma_{He} - \Gamma_r$ with $X = 0.64 \pm 0.05$, confirming the NIST results within uncertainties. (At Wisconsin $\Gamma_r = 1/28.0$ h^{-1} was observed; we are currently determining the source of the decreased value.)

Hence we conclude that in contrast with the result in Ref. [26], we do not observe any non-linear component in the temperature dependence of Γ_{He}. However, based on the maximum observed polarizations of 47 % and 42 % for Jersey and Jekyll, respectively [6], we obtain $X = 1.2 \pm 0.2$. Hence it appears that 100 % Rb polarization may not have been achieved in these cells.

6. Summary

We have successfully fabricated wide angle cells from GE180 glass and achieved lifetimes between 100 h and 400 h. SEOP with diode lasers narrowed by chirped VBGs produced ^{3}He polarization of 65 % - 80% in these cells, as determined by EPR and neutron transmission measurements. Other improvements include a better static field solenoid and lower spin flip losses in the cells. The new wide-angle system will be tested on MACS in early 2013. We have found that our quartz wide-angle cells show the typical linear dependence of relaxation rate on alkali density, but with somewhat high values of X.

7. Acknowledgements

We acknowledge M. Huber for assistance with the neutron transmission measurements on beamline NG6A. This work is supported in part by the U. S. Department of Energy, Basic Energy Sciences and utilized facilities supported in part by the National Science Foundation under Agreement No. DMR-0944772.

References

[1] E. Lelievre-Berna, Physica **397**, 162-167 (2007).
[2] W.C. Chen *et al.*, Physica B **404**, 2663-2666 (2009).
[3] W. Heil *et al.*, Nucl. Instrum. Meth. A **485**, 551-570 (2002).
[4] K.H. Andersen *et al.*, Physica B **404**, 2652-2654 (2009).
[5] C. J. Beecham *et al.*, Physica B **406**, 2429-2432 (2011).
[6] C. B. Fu *et al.*, Physica B **406**, 2419-2423 (2011).
[7] J. A. Rodriguez-Rivera *et al.*, Meas. Sci. Technol. **19**, 034023 (2008).
[8] GE Lighting Component Sales, Bldg. 315D, 1975 Noble Rd., Cleveland, OH 44117. The largest standard GE180 tubing diameter is 16 mm; the 25 mm tubing was procured through a special glass run. Certain trade names and company products are mentioned in the text or identified in an illustration in order to adequately specify the experimental procedure and equipment used. In no case does such identification imply recommendation or endorsement by the National Institute of Standards and Technology, nor does it imply that the products are necessarily the best available for the purpose.
[9] V. Thampy *et al.*, Phys. Rev. Lett. **108**, 107002 (2012).
[10] W.C. Chen *et al.*, Journal of Physics: Conference Series **294**, 012003 (2011).
[11] E. Babcock *et al.*, Phys. Rev. Lett, **91**, 123003, 2003.
[12] G7, McMaster Carr, 200 New Canton Way, Robbinsville, New Jersey 08691-2343.
[13] nLIGHT Corporation, Vancouver, WA.
[14] OptiGrate Corporation, Orlando, Florida.
[15] R.E. Jacob *et al.*, Phys. Rev. A **69** 021401(R) (2004).
[16] G. L. Jones *et al.*, Nucl. Instr. and Meth. in Phys. Res. A **440**, 772-776 (2000).
[17] M. V. Romalis and G. D. Cates, Phys. Rev. A **58**, 3004 (1998).
[18] E. Babcock *et al.*, Phys. Rev. A **71**, 013414 (2005).
[19] B. Chann *et al.*, Phys. Rev. A **66**, 032703 (2002).
[20] Q. Ye, *et al.*, Eur. Phys. J. A **44**, 55-61 (2010).
[21] P. A. M. Dolph *et al.*, Phys. Rev. C **84**, 065201 (2011).
[22] COMSOL Multiphysics, COMSOL, Inc., Los Angeles, CA.
[23] T. J. McKetterick *et al.*, Physica B **406**, 2436-2438 (2011).
[24] USB 6251 DAQ card, National Instruments, Austin, TX.
[25] E. Babcock *et al.*, Phys. Rev. Lett. **96**, 083003 (2006).
[26] T. Ino, S. Muto, Physica B **397** 182 (2007).
[27] W. C. Chen *et al.*, Phys. Rev. A **75**, 013416 (2007).
[28] E. Vliegen *et al*, Nucl. Instrum. Meth. **460**, 444-450 (2001).